Femtosecond versus Nanosecond Surface Photochemistry: O_2+CO on Pt(111) at 80 K

F.-J. Kao,[a] D. G. Busch, D. Gomes da Costa, and W. Ho

Laboratory of Atomic and Solid State Physics and Materials Science Center, Cornell University, Ithaca, New York 14853-2501

(Received 9 April 1993)

Desorption of O_2 and production of CO_2 from O_2 coadsorbed with CO on Pt(111) at 80 K were induced by laser pulses of femtosecond and nanosecond durations. The photoyields with femtosecond pulses show highly nonlinear dependence on fluence, large enhancement of cross section, and increase of the O_2 desorption to CO_2 production branching ratio, when compared with desorption and reaction induced by nanosecond pulses. These differences are attributed to multiple excitations occurring within the time scale of relaxation of the excited adsorbate-surface complex, which are possible with high intensity femtosecond pulse laser irradiation.

PACS numbers: 68.45.Da, 42.65.Re, 78.90.+t, 82.65.−i

In the past few years the desorption of molecules from a solid surface induced by femtosecond laser pulses has been a subject of considerable interest [1–3]. Femtosecond laser pulses not only provide the time resolution necessary for dynamical studies, but also generate highly nonlinear excitations which cannot be easily reached by other means. Highly nonlinear photodesorption yield and enhancement of quantum efficiency have been observed for desorption induced by femtosecond laser pulses of NO from Pd(111) [2,3] and CO from Cu(111) [1]. Multiple excitation of the adsorbed molecules induced by photogenerated hot substrate electrons was determined to be the main mechanism for desorption. However, these studies have been limited so far to desorption of molecules from surfaces, where there are no other competing channels such as dissociation and reaction.

In this Letter we report the first study of surface photoreaction as well as photodesorption induced by femtosecond laser pulses. The system chosen consists of a monolayer of O_2 coadsorbed with CO on Pt(111) at 80 K, $CO/O_2/Pt(111)$. We find that upon irradiation with femtosecond pulses, there is a large amount of O_2 desorption and CO_2 production at 620 nm. In addition, the branching ratio of O_2 desorption to O_2 reacting with CO is increased by more than an order of magnitude when compared with cw and nanosecond pulse excitations. Thus, the hot substrate electron excitation responsible for nonlinear photoyields and enhancement of quantum efficiency also leads to a change in the branching ratio of surface reaction pathways. In previous experiments using cw UV light from an arc lamp, photodesorption and photodissociation of O_2 were observed from $O_2/Pt(111)$ [4, 5]. In addition, CO_2 was formed when $CO/O_2/Pt(111)$ was similarly irradiated [5] or with nanosecond laser pulses [6]. The photoyields were linearly dependent on incident intensity and there was no measurable desorption, dissociation, or reaction for incident photons with wavelengths longer than 550 nm.

The measurements presented here were performed in a UHV chamber equipped with an electron energy loss spectrometer (EELS) and a quadrupole mass spectrometer (UTI 100C). The preparation and characterization of the single crystal Pt(111) were carried out using standard procedures and the cleanliness was checked with EELS and temperature programmed desorption (TPD) [5]. The sample was held at a base temperature of 80 K, and was dosed by a microcapillary array with O_2 first and then CO, both to saturation coverage. At 80 K oxygen is known to chemisorb molecularly on Pt(111) as two different species, a bridge site and an atop site which are characterized by different O-O stretch frequencies [7–9], while CO occupies only atop sites [5].

An amplified colliding-pulse mode-locked laser operating at 10 Hz and 620 nm provided femtosecond pulses of different durations [10]. The beam was collimated on the sample to form a spot size of 2 mm^2. Autocorrelation performed by second harmonic generation on the sample surface typically gave a pulse width of 150–180 fs with energy per pulse in the range of 50 to 70 μJ. Longer laser pulses were generated by chirping femtosecond pulses to 600 fs. The 310 nm pulses were obtained by frequency doubling 620 nm pulses in a β-barium borate crystal. A Q-switched Nd:YAG laser provided 3 ns, 355 nm pulses at 10 Hz. All the laser pulses entered and exited the UHV chamber at 28° from the sample surface normal. Desorbed molecules were detected normal to the sample surface by the mass spectrometer operating in pulse counting mode. Background counts were minimized by gating the pulse counting electronics and by using isotopic $^{18}O_2$ and $^{13}C^{18}O$.

Femtosecond and nanosecond laser desorption signals of O_2 from $CO/O_2/Pt(111)$ as a function of cumulative photon fluence are shown in Fig. 1. The average fluence of the nanosecond pulses is 6 mJ/cm^2 at 355 nm, while that of the femtosecond pulses is 2 mJ/cm^2 at 310 nm. The raw data from femtosecond pulse excitation, after background subtraction, are iteratively normalized to the power law of fluence and are fitted to a decaying signal given by

$$N_{1,i}=N_{\mathrm{raw},i}(F_{\mathrm{avg}}/F_i)^P, \tag{1}$$

and

$$N_1=a_1e^{-F_{\mathrm{avg}}\sigma_{1i}}+a_2e^{-F_{\mathrm{avg}}\sigma_{2i}}, \tag{2}$$

where F_i is the fluence of the ith pulse, F_{avg} is the average

0031-9007/93/70(26)/4098(4)$06.00

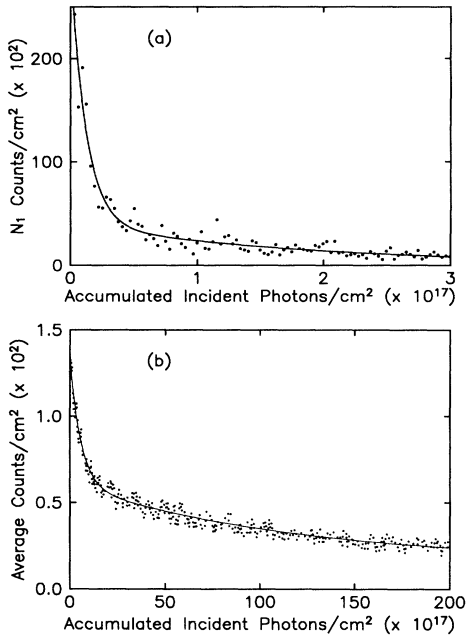

FIG. 1. $^{18}O_2$ desorption signals from $^{13}C^{18}O/^{18}O_2/Pt(111)$ at 80 K: (a) Desorption with 310 nm, 150 fs pulse. Each point represents fluence normalized desorption count per illuminated area, according to Eq. (1). The desorption signal is fitted to a double exponential decay (solid curve) as described by Eq. (2), where σ_1 represents the effective cross section, $\sigma_1 > \sigma_2$. (b) desorption with 355 nm, 3 ns pulse. The counts are not normalized to the laser pulse fluence, since the pulse to pulse fluctuation is less than 2% and the yield is proportional to the fluence. The desorption signal is also fitted to a double exponential decay (solid curve) as described by Eq. (2), where σ_1 and σ_2 represent the fast and slow effective cross sections, respectively.

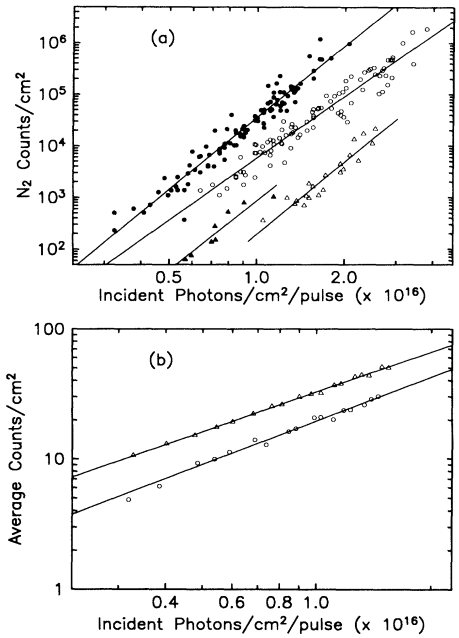

FIG. 2. Dependence of yields on pulse fluence for $^{18}O_2$ desorption and $^{13}C^{18}O_2$ production from $^{13}C^{18}O/^{18}O_2/Pt(111)$ at 80 K: (a) 150 and 600 fs laser pulses at 620 nm. The counts, $N_{2,i}$, are normalized to the decaying signals according to Eq. (3) before they are plotted. Solid (●) and open (○) circles correspond to $^{18}O_2$ desorption counts induced by a single 150 and a single 600 fs laser pulse, respectively, while solid (▲) and open (△) triangles correspond to $^{13}C^{18}O_2$ desorption counts induced by a single 150 and a single 600 fs laser pulse, respectively. Solid lines are best fits to the data. (b) 3 ns laser pulses at 355 nm for $^{18}O_2$ (○) and $^{13}C^{18}O_2$ (△). Each data point represents an average of counts from ~100 pulses at the given fluence.

photon fluence per pulse, and P is the power law exponent. The decaying signal is generally fitted to the sum of two exponentials to reflect the depleting surface coverage. However, only one of the fitting parameters, σ_1 of the fast decay component, is used to represent the effective cross section for desorption, dissociation, and reaction of O_2, since the other parameter, σ_2, is mainly fitted to counts close to the background. The best fit yields $\sigma_1 = 1.2\times10^{-16}$ cm^2, $\sigma_2 = 5\times10^{-18}$ cm^2, and $P=3$ for the data shown in Fig. 1(a).

The O_2 depletion signal induced by nanosecond pulses from $CO/O_2/Pt(111)$ is illustrated in Fig. 1(b). The effective cross sections σ_1 and σ_2 obtained from a fit by Eq. (2) are 1.7×10^{-18} and 8×10^{-20} cm^2, respectively. The need for two exponentials suggests that there are at least two types of photoactive O_2 species. The slow cross section σ_2 is in good agreement with those obtained in arc lamp experiments [4,5], while the fast cross section σ_1 is comparable to the CO_2 production cross section measured previously with nanosecond laser pulses at 308 nm [6].

The comparison of the fluence dependence of the yields for nanosecond and femtosecond pulses is shown in Fig. 2. The fluence dependence of O_2 and CO_2 yields N_2 for femtosecond pulses at 620 nm is shown in Fig. 2(a). The counts are normalized to the decay of the signal,

$$N_{2,i} = N_{\mathrm{raw},i}\left(\frac{a_1 e^{-F_{\mathrm{avg}}\sigma_1 i} + a_2 e^{-F_{\mathrm{avg}}\sigma_2 i}}{a_1 + a_2}\right)^{-1}, \qquad (3)$$

before they are plotted for each laser pulse in order to factor out the irreversible changes caused by previous pulses. The superlinear power factor P is obtained from the best fit to the log-log plot. The pulse fluence was varied by using neutral density filters and by taking advantage of the pulse-to-pulse fluence fluctuations (~20%). The photoyields of O_2 and CO_2 are displayed in Fig. 2(b) as a function of laser pulse fluence for nanosecond pulses at 355 nm. The yields are essentially linear in the fluence, $N_2 \sim F^{1.11\pm0.05}$ for O_2 and $N_2 \sim F^{1.01\pm0.05}$ for CO_2.

Under femtosecond laser pulse excitation, the effective desorption and reaction cross sections are enhanced by approximately 2 orders of magnitude when compared with nanosecond pulse excitation and the dependence of yield on fluence is highly nonlinear. In addition, the

desorption/reaction branching ratios increase by more than an order of magnitude compared to nanosecond pulse excitation. Regardless of the mechanism, the branching ratio is determined by taking the ratio of counts of O_2 to CO_2 at a fixed fluence; it is relatively independent of the fluence shown in Fig. 2. Substantial increase in the ratio is observed for femtosecond pulse excitation, as shown in Table I. The nonlinear yield dependence on fluence and the enhancement of cross sections obtained are similar to those observed in previous studies of femtosecond laser desorption [1,3]. Therefore, the significant increase in the branching ratio of O_2 desorption to the reaction with CO suggests that ultrashort pulses also lead to a change in the kinetics of surface photochemistry.

Surface photochemistry of O_2 on Pt(111) [5,6] induced by cw light sources has been attributed to an electronic excitation of the adsorbate-substrate complex within the model of desorption induced by electronic transitions (DIET) introduced by Menzel, Gomer, and Redhead [11]. The incident photon causes a Franck-Condon transition from the ground state potential energy surface (PES) to an excited state PES. The adsorbate acquires kinetic energy in the excited state PES before being quenched down to the ground state PES. Desorption, dissociation, or reaction results if the adsorbate remains in the excited state long enough to gain sufficient energy.

For femtosecond laser pulse excitations, the nonlinear fluence dependence rules out the mechanism being a one-photon process. Processes involving direct multiphoton excitation of the adsorbate-substrate complex may also be ruled out, since in two-pulse correlation measurements of O_2 desorption from O_2/Pt(111), in which the desorption signal is measured as a function of the time delay between the two laser pulses, the full width at half maximum of the time scale for the desorption signal is 1.2 ps [12]. The time scale is about 8 times longer than the laser pulse width, indicating that the excitations leading to desorption remain effective for time periods longer than the laser pulse duration.

In previous studies of femtosecond laser desorption, it was assumed that the desorption was mainly driven by hot substrate electrons, which thermalized with each other at an electron temperature T_e of a few thousand degrees before the lattice had a chance to heat up [1,13–15]. Furthermore, it was found in state-resolved measurements that the desorbed molecules have a vibrational distribution characterized by $T_v \approx 2200$ K and the translational energy distribution described by a temperature of ≈ 600 K [2]. A "friction" model based on direct coupling between the center-of-mass degree of freedom of the adsorbate and the electron-hole pair excitations of the substrate was proposed to explain the high temperature of vibrational distribution and the lower temperature of translational energy distribution [16]. In this model, the electronic friction coefficient, which is related to the vibrational linewidth of the adsorbate, determines the strength of coupling and reaction rates follow the electronic temperature with an Arrhenius-like dependence. However, the friction model leads to a considerably longer time scale for the desorption signal from two-pulse correlation measurements, unless the electronic friction coefficient is chosen to be unreasonably large [16]. In addition, high temperature vibrational distribution was found even for nanosecond pulse desorption [17], where the mechanism of adsorbate excitation cannot be frictional coupling because the yield is linear in fluence and thus nonthermal in T_e.

A generalized DIET scheme [18], desorption induced by multiple electronic transitions (DIMET), was thus proposed for femtosecond excitation in order to resolve the time scale problem encountered by the friction model. In the simple DIET model, if the adsorbate remains in the excited state PES for a time shorter than a critical duration τ_c, it returns to the ground state PES without desorbing; however, it may remain vibrationally excited for a few vibrational periods. In DIMET, the vibrationally excited adsorbate can be excited repeatedly by hot substrate electrons, increasing the overall time spent in the excited PES. Thus, the probability for desorption is greatly enhanced. In this way, a superlinear fluence dependence of the yield and an enhancement of the cross

TABLE I. Comparison of TPD, nanosecond pulse irradiation, and femtosecond pulse irradiation of O_2 desorption and the branching ratio for O_2 desorption/CO_2 production from CO/O_2/Pt(111) at 80 K.

	TPD	3 ns 355 nm	600 fs 620 nm	600 fs 310 nm	150 fs 620 nm	150 fs 310 nm
Typical fluence		6 mJ/cm^2	5 mJ/cm^2	2 mJ/cm^2	3 mJ/cm^2	2 mJ/cm^2
O_2 yield vs fluence		Linear	$Y \sim F^{4.5\pm0.5}$	$Y \sim F^{3\pm0.5}$	$Y \sim F^{5.5\pm0.7}$	$Y \sim F^{3\pm0.5}$
Mechanism	Phonons	Single photon	Multiple photon	Multiple photon	Multiple photon	Multiple photon
Effective[a] cross section (cm^2)		1.7×10^{-18} (fast) 8×10^{-20} (slow)	2×10^{-17}	5×10^{-17}	5.5×10^{-17}	1.2×10^{-16}
Branching ratio[b] of O_2/CO_2	45 (from 80 to 200 K)	0.5	20 ± 8	10 ± 5	30 ± 10	15 ± 5

[a]Effective cross sections for the multiple photon processes are given at the typical fluence and have an uncertainty of approximately 50%.

[b]Values listed were not corrected for differences in mass spectrometer sensitivity for O_2 and CO_2.

section for O_2 desorption compared to nanosecond excitation can be explained [12,18]. Each excitation-deexcitation cycle in the DIMET process only transfers a small amount of vibrational energy because the lifetime in the excited state PES is very short, on the order of a few femtoseconds. Such an excitation process is similar to thermal desorption except that hot substrate electrons instead of phonons act as the excitation source. The DIMET process in a way lies in between the thermally equilibrated thermal desorption and the nonthermal DIET process. If the excited adsorbate returns to the ground state and dissipates all excess vibrational energy before being excited again, the DIMET process simply reduces to the DIET process. However, if multiple excitation-deexcitation cycles occur within the time scale of relaxation of the excited adsorbate-substrate complex, a DIMET process may resemble that of thermal desorption.

On Pt(111) at 80 K, oxygen adsorbs either as O_2^{-1} (superoxo) [19] or O_2^{-2} (peroxo) [7] and the binding energy of adsorbed oxygen molecules is $E_{\rm des}=380$ meV, while the activation energy for dissociation is $E_{\rm dis}=340$ meV [7,20,21]. The mechanism for forming CO_2 may involve reaction of hot O atoms with CO and/or excited O_2 reacting with CO. If oxygen dissociation is the precursor to CO_2 production, as in the hot oxygen atom mechanism [5], the branching ratio of O_2 desorption to CO_2 production, R_B, is given by $R_B \propto e^{-(E_{\rm des}-E_{\rm dis})/kT}$. In TPD measurements, R_B is about 45 when the yields are integrated from 80 to 200 K. The higher effective temperature ($T=T_e\sim 1500$ K) in the DIMET process should lead to a larger branching ratio (>45), contrary to experimental observations. The smaller branching ratio R_B for DIMET compared to TPD would, however, be consistent with a higher activation energy for CO_2 production compared to O_2 desorption. The activation energy for CO_2 production can thus be estimated to be about 6 meV higher than the desorption activation energy from the measured branching ratios of 45 for TPD and 30 for femtosecond pulse irradiation at 620 nm with 150 fs duration. These results suggest a mechanism for the production of CO_2 which involves the reaction of a photoexcited molecular oxygen with coadsorbed CO [6]. The reaction between coadsorbed molecular oxygen and CO has also been proposed for thermally induced reactions [22,23].

Support of this research by the Office of Naval Research under Grant No. N00014-90-J-1214 and the Department of Energy under Grant No. DE-FG02-91-ER14205 is gratefully acknowledged. In addition, the authors would like to thank F. M. Zimmermann for invaluable contributions and J. A. Misewich for illuminating discussions.

[a]Present address: Physics Department, National Sun Yat-Sen University, Kaohsiung, Taiwan, Republic of China.

[1] A. Prybyla, H. W. K. Tom, and G. D. Aumiller, Phys. Rev. Lett. **68**, 503 (1992).
[2] J. A. Prybyla *et al.*, Phys. Rev. Lett. **64**, 1537 (1990).
[3] F. Budde *et al.*, Phys. Rev. Lett. **66**, 3024 (1991).
[4] X.-Y. Zhu *et al.*, J. Chem. Phys. **91**, 5011 (1989).
[5] W. D. Mieher and W. Ho, J. Chem. Phys. **91**, 4755 (1989); (to be published).
[6] V. A. Ukraintsev and I. Harrison, J. Chem. Phys. **96**, 6307 (1992).
[7] J. L. Gland, B. A. Sexton, and G. B. Fisher, Surf. Sci. **95**, 587 (1980).
[8] N. R. Avery, Chem. Phys. Lett. **96**, 371 (1983).
[9] H. Steininger, S. Lehwald, and H. Ibach, Surf. Sci. **123**, 1 (1982).
[10] F. J. Kao, Ph.D. thesis, Cornell University, 1993.
[11] D. Menzel and R. Gomer, J. Chem. Phys. **41**, 3311 (1964); P. A. Redhead, Can. J. Phys. **42**, 886 (1964).
[12] F. J. Kao *et al.* (to be published).
[13] H. E. Elsayed-Ali *et al.*, Phys. Rev. Lett. **58**, 1212 (1987).
[14] P. B. Corkum, F. Brunel, and N. K. Sherman, Phys. Rev. Lett. **61**, 2886 (1988).
[15] R. W. Schoenlein *et al.*, Phys. Rev. Lett. **58**, 1680 (1987).
[16] D. M. Newns, T. F. Heinz, and J. A. Misewich, Prog. Theor. Phys. **106**, 411 (1991).
[17] M. Asscher *et al.*, J. Chem. Phys. **96**, 4808 (1992).
[18] J. A. Misewich, T. F. Heinz, and D. M. Newns, Phys. Rev. Lett. **68**, 3737 (1992).
[19] D. A. Outka *et al.*, Phys. Rev. B **35**, 4119 (1987).
[20] A. C. Luntz, M. D. Williams, and D. S. Bethune, J. Chem. Phys. **89**, 4381 (1988).
[21] C. T. Rettner and C. B. Mullins, J. Chem. Phys. **94**, 1626 (1991).
[22] T. Matsushima, Surf. Sci. **127**, 403 (1983).
[23] A. J. Capote, J. T. Roberts, and R. J. Madix, Surf. Sci. **209**, L151 (1989).